Dendrochronologia 58 (2019) 125650

Contents lists available at ScienceDirect

Dendrochronologia

journal homepage: www.elsevier.com/locate/dendro

Ongoing modifications to root system architecture of *Pinus ponderosa* growing on a sloped site revealed by tree-ring analysis

Antonio Montagnoli[a,*], Mattia Terzaghi[a], Donato Chiatante[a], Gabriella S. Scippa[b], Bruno Lasserre[b], R. Kasten Dumroese[c]

[a] Department of Biotechnology and Life Science, University of Insubria, Via Dunant, 3 – 21100 Varese, Italy
[b] Department of Biosciences and Territory, University of Molise, Contrada Fonte Lappone, Pesche, Italy
[c] Rocky Mountain Research Station, U.S. Department of Agriculture Forest Service, 1221 South Main Street, Moscow, ID 83843, USA

ARTICLE INFO

Keywords:
Root system architecture
Tree anchorage
Mechanical forces
Lateral root emission
Compression wood
Annual tree ring

ABSTRACT

Our knowledge of the root system architecture of trees is still incomplete, especially concerning how biomass partitioning is regulated to achieve an optimal, but often unequal, distribution of resources. In addition, our comprehension of root system architecture development as a result of the adaptation process is limited because most studies lack a temporal approach. To add to our understanding, we excavated 32-year-old *Pinus ponderosa* trees from a steep, forested site in northern Idaho USA. The root systems were discretized by a low magnetic field digitizer and along with AMAPmod software we examined their root traits (i.e. order category, topology, growth direction length, and volume) in four quadrants: downslope, upslope, windward, and leeward. On one tree, we analyzed tree rings to compare the ages of lateral roots relative to their parental root, and to assess the occurrence of compression wood. We found that, from their onset, first-order lateral roots have similar patterns of ring eccentricity suggesting an innate ability to respond to different mechanical forces; more root system was allocated downslope and to the windward quadrant. In addition, we noted that shallow roots, which all presented compression wood, appear to be the most important component of anchorage. Finally, we observed that lateral roots can change growth direction in response to mechanical forces, as well as produce new lateral roots at any development stage and wherever along their axis. These findings suggest that trees adjust their root spatial deployment in response to environmental conditions, these roots form compression wood to dissipate mechanical forces, and new lateral roots can arise anywhere and at any time on the existing system in apparent response to mechanical forces.

1. Introduction

A comprehensive knowledge of the complex root phenome (i.e. its structure and function; Atkinson et al., 2019) of a plant helps develop a better understanding of important aspects of the root's behavior regarding water and nutrient absorption, anchorage, carbohydrate storage, and deposition and excretion of biochemical compounds (Danjon et al., 2013; Pagès, 2002; Terzaghi et al., 2016). A complete understanding of root properties becomes essential for woody species (shrubs and trees) as they live longer and achieve larger dimensions than their non-woody cohorts. The weight of woody, above-ground organs is considerable and the resulting, powerful mechanical forces need to be dissipated into the soil to avoid uprooting (Stokes and Mattheck, 1996).

Our understanding of root system architecture (RSA) in trees and shrubs relies heavily on studies using the shovelomic approach (that being a time-consuming, labor-intensive, destructive approach where a complete root system is excavated by hand), accomplished by using one of several principal methods (Chiatante et al., 2019; Colombi et al., 2015; Dumroese et al., 2019; Montagnoli et al., 2019). After excavation, coarse roots are manually mapped to measure traits such as the number, length, volume, surface area, and topological location of all lateral roots (classified according to their branching order) and wood density (Iyer-Pascuzzi et al., 2010), often assessed with regard to soil depth and volume and stand density (Böhm, 1979).

A long term aim of RSA studies is to underpin development of *in silico* predictive models able to foresee the plant response in its root system when environmental changes occur (Yang et al., 2016). These models could assist in development of next-generation planting

* Corresponding author.
E-mail addresses: antonio.montagnoli@uninsubria.it (A. Montagnoli), mattia.terzaghi@uninsubria.it (M. Terzaghi), donato.chiatante@uninsubria.it (D. Chiatante), scippa@unimol.it (G.S. Scippa), lasserre@unimol.it (B. Lasserre), kas.dumroese@usda.gov (R.K. Dumroese).

https://doi.org/10.1016/j.dendro.2019.125650
Received 30 July 2019; Received in revised form 17 October 2019; Accepted 25 October 2019
Available online 04 November 2019

material that is more resilient to predicted climate change or simply be the modeling basis to provide a more realistic measurement of the amount of carbon stored as perennial roots (coarse structural roots) in forest ecosystems (King et al., 1996). Currently, however, knowledge of how RSA develops is still incomplete, and one aspect that needs to be understood is how biomass partitioning is regulated because the anchorage strength of a tree depends upon an optimal distribution of resources (Stokes and Mattheck, 1996). Indeed, if wood is laid down with a greater density at areas of mechanical stress, then the possibility to tolerate such stress increases (van Gelder et al., 2006; Chave et al., 2009; Anten and Schieving, 2010). This fact explains why root biomass allocation is not normally evenly distributed. On one hand, the literature suggests that the RSA may undergo variations throughout different developmental stages that characterize the growth cycle of a plant or in response to abiotic factors, such as wind, slope, and soil conditions that threaten its anchorage (Schroth, 1998; Puhe, 2003; Stokes et al., 2009; Ji et al., 2012; Ghestem et al., 2011). On the other hand, the literature also suggests that some tree species, such as *Pinus pinaster*, are unable to regenerate an appropriate spatial arrangement of main structural roots from a defective juvenile RSA that lacks some major anchorage component (Danjon et al., 2005).

The lack of a temporal approach in RSA studies that could reveal the chronology of lateral root formation limits our ability to describe the steps leading to a particular RSA development as the result of the adaptation process. Therefore, understanding the chronological sequence of lateral root emission in different zones surrounding the taproot could help unveil why RSA has changed during the lifespan of the tree as it grows to achieve a higher functional performance. Moreover, the analysis of a temporal factor could improve the reliability of two- and three-dimensional (2D and 3D) provisional models (reviewed in Dupuy et al., 2010) and leverage mechanistic studies where factors responsible for deployment of a certain type of RSA are investigated.

In addition to root deployment, the type of wood residing in the roots is undoubtedly important. Unlike the stem, occurrence of wood modification in roots has been poorly explored despite the occurrence of asymmetric annual rings and specialty roots (e.g. I- and T-beam) reported in both gymnosperms (Coutts et al., 1999; Dumroese et al., 2019; Fourcaud et al., 2008; Ghani et al., 2009) and angiosperms (De Zio et al., 2016; Di Iorio et al., 2005). Mechanical stress induced by stem sway has been suggested as the cause of annual rings at the root-stem base that are wider than those elsewhere on the root system (Fayle, 1975, 1976). This asymmetric growth could play an important role in increasing root stiffness with the consequent effect of reinforcing mechanical anchorage of a tree.

In cross section, the portion of wood showing an eccentricity of the annual rings and often a different coloring is defined as reaction wood. Ring eccentricity is the consequence of a different number of cell layers distributed around the circumference of the annual rings (Kim et al., 2016), whereas different coloring is due to a variation in the chemical and physical organization of the cell walls (Ruelle, 2014). Gravity is a major factor responsible for inducing reaction wood formation (Du and Yamamoto, 2007). In gymnosperms, reaction wood is termed compression wood and forms in the opposite direction of the mechanical stress (Westing, 1965; Alméras and Clair, 2016). Compression wood typically appears as wide, crescent-shaped bands of darker brown wood that sometimes resembles latewood, the darker colored, outer part of growth rings, although the cells are different (Donaldson and Singh, 2016). In an inclined stem of a gymnosperm tree growing on a level site, compression wood forms normally on the lower side in response to gravity (i.e. inertial force), but in *Tsuga mertensiana* (references in Westing, 1965), compression wood was observed in response to the presence of a slope, or on the lee side when a tree was bent by constant directional wind. In angiosperms, reaction wood is termed tension wood, and the annual ring eccentricity is visible in the opposite direction as that found in gymnosperms (Westing, 1965). At the cytological level, compression wood is formed by a single tissue with a type of cells (tracheid) playing both a nutritional and mechanical role, whereas in tension wood these two functions are entrusted upon different cell types, such as vascular, mechanical, and parenchyma. The formation of reaction wood in roots is, however, little explored (Hathaway and Penny, 1975) except in response to soil erosion (Gärtner, 2007; Hitz et al., 2008; Wistuba et al., 2013) or bending (De Zio et al., 2016).

Toward improving our understanding of root spatial deployment, we investigated root traits of a shrub (*Spartium junceum*, Lombardi et al., 2017), angiosperm trees (*Quercus cerris*, Di Iorio et al., 2007; *Quercus pubescens*, Di Iorio et al., 2005), and a gymnosperm tree (*Pinus ponderosa*, Dumroese et al., 2019). In these studies we found that plants growing on slopes adapt their RSA to achieve stronger anchorage to the soil. Such reinforcement is achieved through the deployment of an asymmetric distribution of lateral roots surrounding the stump. Here we continue this series of shovelomic studies by describing a number of aspects of the RSA in *P. ponderosa* trees growing 32 years on a steep slope. Our hypotheses are that 1) environmental conditions (e.g. wind, slope conditions, soil hydrology) require adjustments of root spatial deployment, and 2) that continuous variability in conditions (e.g. changes in self-loading weight of shoots occurring during plant growth) require that, to satisfy mutable needs, the root biomass distribution changes in time and space by either the emission of new laterals and production of compression wood. Therefore, we used two analytical approaches to examine root length and volume in different root ordering in four quadrants surrounding the stump (downslope, upslope, windward, and leeward); furthermore, employing a tree-ring analysis, we investigated the chronological sequence of root development and explored the formation of compression wood in different root orders and along the roots axis.

2. Materials and methods

2.1. Site description, tree establishment, excavation, and 3-dimensional measurement

Typical forested sites occurring on the northern Rocky Mountains in northern Idaho, USA are comprised of mixed conifer species that reflect a wildfire-based disturbance regime; one dominant conifer species is *Pinus ponderosa*. Our sampled trees were growing on a typical forest site at about 1000 m elevation on the University of Idaho Experimental Forest in northern Idaho (lat. 46.842240, long. −116.871035) on a northeast aspect (Fig. 1), and were collected as part of another study because of the known history of the trees. The site has slopes of 30 to 50% and the deep (~1.5 m) soil was derived from volcanic ash above weathered granite (Vassar series, Typic Udivitrands, Andisol; Soil Survey Staff, 2013). This soil type is characterized by a low cohesive friction (Johnson et al., 2007). Ecologically, the site is classified as a *Thuja plicata/Clintonia uniflora/Clintonia uniflora* phase habitat type (Cooper et al., 1987). In 1985, the forest was clearcut and the slash was broadcast burned during autumn 1985 to facilitate outplanting and reduce wildfire risk. In March 1986, one-year-old nursery seedlings of *P. ponderosa* grown in 60-ml containers following the growing regime of Wenny and Dumroese (1987) were hand-planted on a 2-m (between rows) × 1-m (within rows) spacing as part of an experiment (see Wenny et al., 1988). During autumn 1986, every other seedling was sampled leaving residual trees on a 2- × 2-m spacing. Weather data from the nearest stations (7 to 16 km) to the study site are shown in Table 1. The prevailing wind is west southwest during the growing season (Western Regional Climate Center, 2019). Similar sites have ~100 frost-free days per year (Soil Survey Staff, 2013). No irrigation, fertilization, weeding, or thinning was done after outplanting.

In early July 2017, we relocated the *P. ponderosa* trees. We randomly selected 15 trees to assess diameter breast height (DBH) measured cross slope, height, and canopy projected area (Table 2), and mapped their locations in relation to other nearby trees (Fig. 1). Of these, 10 trees were randomly selected for excavation and of these, 8

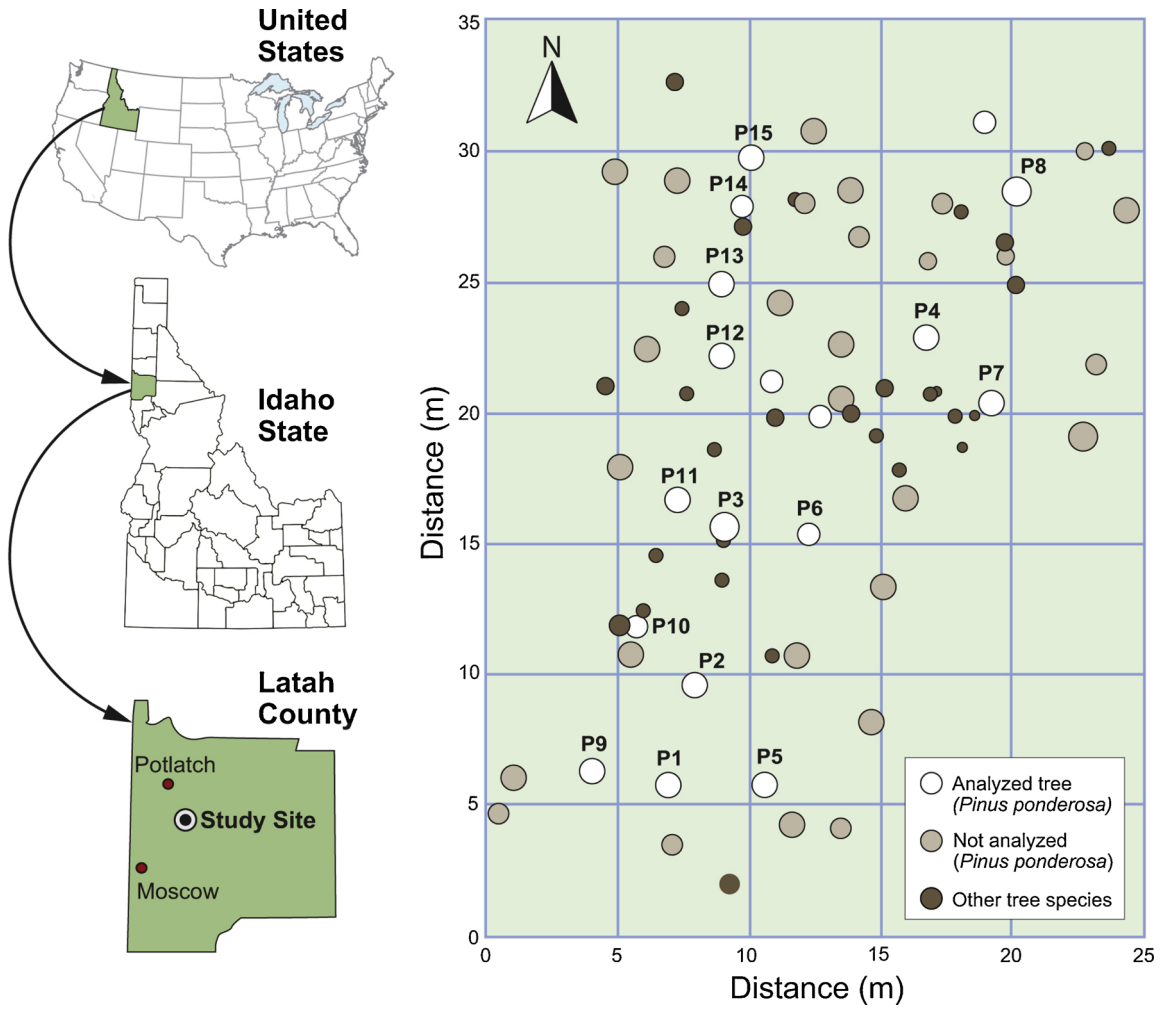

Fig. 1. Location of the study site in northern Idaho, USA, and locations of the sampled trees and nearby trees.

were digitized. See Dumroese et al. (2019) for complete details on root excavation and digitization. Briefly, to excavate the roots, we felled trees, marked stumps, and removed the soil with an air-spade. Root systems were brought to the laboratory, repositioned to their original orientation, and digitized using a low magnetic digitizer, transmitter, and receiver. Data were encoded in a standard format (MTG) commonly used for representing branching topological (i.e. branching hierarchic structure) relationships (Godin and Caraglio, 1998). The topology was coded according to the "acropetal-development approach" (Danjon et al., 2013; Sorgonà et al., 2018) with the seed-origin radicle, the

Table 1
Weather data collected near the study site (Western Regional Climate Center, 2019).

Month	Air temperature[a]		Precipitation[a]	Snowfall[a]	Wind[b]	
	Maximum (°C)	Minimum (°C)	(mm)	(cm)	Direction	Speed (km/h)
Jan	2.2	−6.1	72	38.4	E	14.6
Feb	5.3	−4.0	61	19.8	E	13.7
Mar	8.9	−2.1	61	11.4	E	14.2
Apr	13.9	0.4	51	3.0	SW	12.6
May	18.9	3.3	54	0.3	WSW	11.6
Jun	22.6	6.2	48	0.0	WSW	9.8
Jul	28.2	7.7	20	0.0	WSW	7.6
Aug	28.3	6.8	20	0.0	WSW	8.2
Sep	23.0	3.8	33	0.0	WSW	8.8
Oct	15.8	0.6	48	0.8	E	10.6
Nov	7.3	−1.9	75	12.4	E	13.8
Dec	2.9	−4.9	79	29.0	E	15.0
Average	14.8	0.8	–	–	–	11.7
Average total	–	–	622	115.1	–	–

[a] Data from 1915 to 2016 (Potlatch 3 NNE [107301]).
[b] Data from 1996 to 2006 (Pullman–Moscow Regional Airport).

Table 2
Characteristics of sampled trees.

Tree	Canopy projected area[a] (m^2)	DBH[b] (cm)	Height (m)
P1	8.0	24.1	16.8
P2	4.4	24.8	17.0
P3	12.5	29.1	17.9
P4	11.1	24.1	15.2
P5	9.7	25.6	16.0
P6	9.9	23.3	17.1
P7	7.2	27.7	17.3
P8	31.9	34.2	16.2
P9	15.8	27.8	19.0
P10	10.7	19.6	16.5
P11	13.6	27.1	18.2
P12	5.5	21.4	14.9
P13	11.1	28.6	19.8
P14	4.6	19.3	17.5
P15	13.9	23.1	20.1
Mean ± standard deviation	11.3 ± 6.6	25.3 ± 3.9	17.4 ± 1.5

[a] Canopy projected area was estimated by measuring from the stem outward to the edge of the canopy at 8 points around the tree: N, NW, W, SW, S, SE, E, and NE.
[b] Diameter breast height measured cross slope.

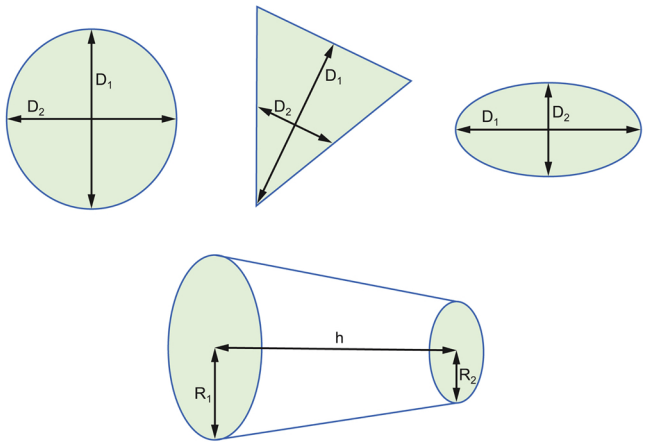

Fig. 2. Root segment volume was estimated using Eq. 1 for a truncated cone. Independent of orientation, the longest diameter (D_1) and the diameter perpendicular to the D_1 midpoint (D_2) were measured at each segment end. The average radius for each segment end (R_1 and R_2) was calculated as the average of D_1 and D_2 for each corresponding segment end.

primary roots (-axis) or taproot designated order zero (pink color in Fig. 3). Lateral roots emerging from the taproot were designated first-order roots (green color in Fig. 3), with second-order roots then originating from these first-order laterals (blue color in Fig. 3), and so on (Zobel and Waisel, 2010). We measured all roots having a proximal diameter ≥ 1 cm at the base.

We used AMAPmod software (Godin et al., 1997) to analyze the data, and computed root traits (i.e. length, diameter, and volume) from the 3-dimensional (3D) digitizing data of entire root systems. We analyzed data by four quadrants, considering root traits as a function of up- versus down-slope direction and of west- (windward) versus east- (leeward) direction, with the downslope direction coinciding with north and the west-east axis coinciding with the direction of the prevailing wind. Moreover, the analysis was repeated at two depths: 0–30 cm (where zero coincides with the soil surface) and 30–60 cm with a maximum depth of ~1.5 m. See Dumroese et al. (2019) for more details.

2.2. Root system architecture

We followed the modified terminology suggested by Danjon et al. (2013) for *P. pinaster*. Our observations focused on the shallow roots branching from the upper portion of the taproot and that are characterized by an axis where the first portion shows a very rapid taper (i.e. "zone of rapid taper"). We use the term "sinker" to indicate lateral roots that grow straight downward independent of their branching order. Based on Danjon et al. (2005), the term "cage" was used to define a cylindrical zone surrounding the taproot and having a diameter of 2.2 × DBH (stem diameter at breast height, ~ 1.3 m), which is comprised of most of the sinker roots along with the taproot and part of the shallow coarse roots.

Using AMAPmode software, a lateral root that is emitted from one quadrant (i.e. downslope, upslope, windward, and leeward) but changes direction and grows into another quadrant has the relative portions of its traits assigned to both quadrants. In addition to this AMAPmode quadrant (AQ) approach, we also manually traced first- and second-order lateral roots back to their junction points with the taproot; we termed this point of initiation the emission quadrant (EQ). For example, if a first-order lateral root had its junction in the downslope quadrant of the taproot, all subsequent roots (second- and third-order) emanating from it were also assigned to the downslope quadrant, regardless of whether or not the roots subsequently grew into other quadrants. For each emission quadrant, length and volume of roots were determined by dividing roots into segments of 10 to 30 cm length from their point of attachment to the parental root. On each end of the segment, we measured the largest diameter (D_1; Fig. 2). From the midpoint of D_1 we measured the diameter perpendicular to it (D_2) and calculated an average diameter and an average radius. The average radius for each segment end (R_1 and R_2) and the length of the segment (h) was used to calculate the segment volume as a truncated cone:

$$V = 1/3\pi\,(R_1^2 + R_1R_2 + R_2^2)\,h \quad (1)$$

and total volume and total length of each lateral root was the sum of the all segment values. We also determined the cross sectional area (CSA) of the first-order lateral root where it met the taproot using the following formula:

$$CSA = D_1 \times D_2 \times \pi \quad (2)$$

where D_1 and D_2 are as described above.

2.3. Tree-ring analysis

One root system was randomly selected for detailed analysis. We divided the taproot axis into three sectors (0–30 cm; 30–60 cm; > 60 cm) because our previous work (Dumroese et al., 2019) showed that all the shallow lateral roots originated in the first 30 cm of the taproot axis and almost all the remaining lateral roots originated between 30–60 cm. We cut each lateral root at its respective branching point with a higher order root. At the branching point, we cut a 3-cm-thick cross section, polished it with a belt sander using progressively finer grits of sandpaper (60, 80, 120, 150, 220, 300, up to 600 grit), and then counted the number of annual rings with the aid of an Olympus microscope (BX41). We cross-dated each sample using the list year technique in which tree rings were counted backwards from the known year of felling (2017). Ring-dating of root sections presenting a number of discontinuous annual rings was accomplished using a modification of the Zig-Zag Segment Tracing Method (Wrońska-Wałach et al., 2016). We observed that the discontinuous annual rings were always oriented in a single direction and therefore it was possible to divide the root section into four sectors with perpendicular radii placed to ensure one radius had maximum length. The radius with the greatest number of growth rings was selected (Krause and Morin, 1995). Although growth rings were usually measured along the radius, we deviated when

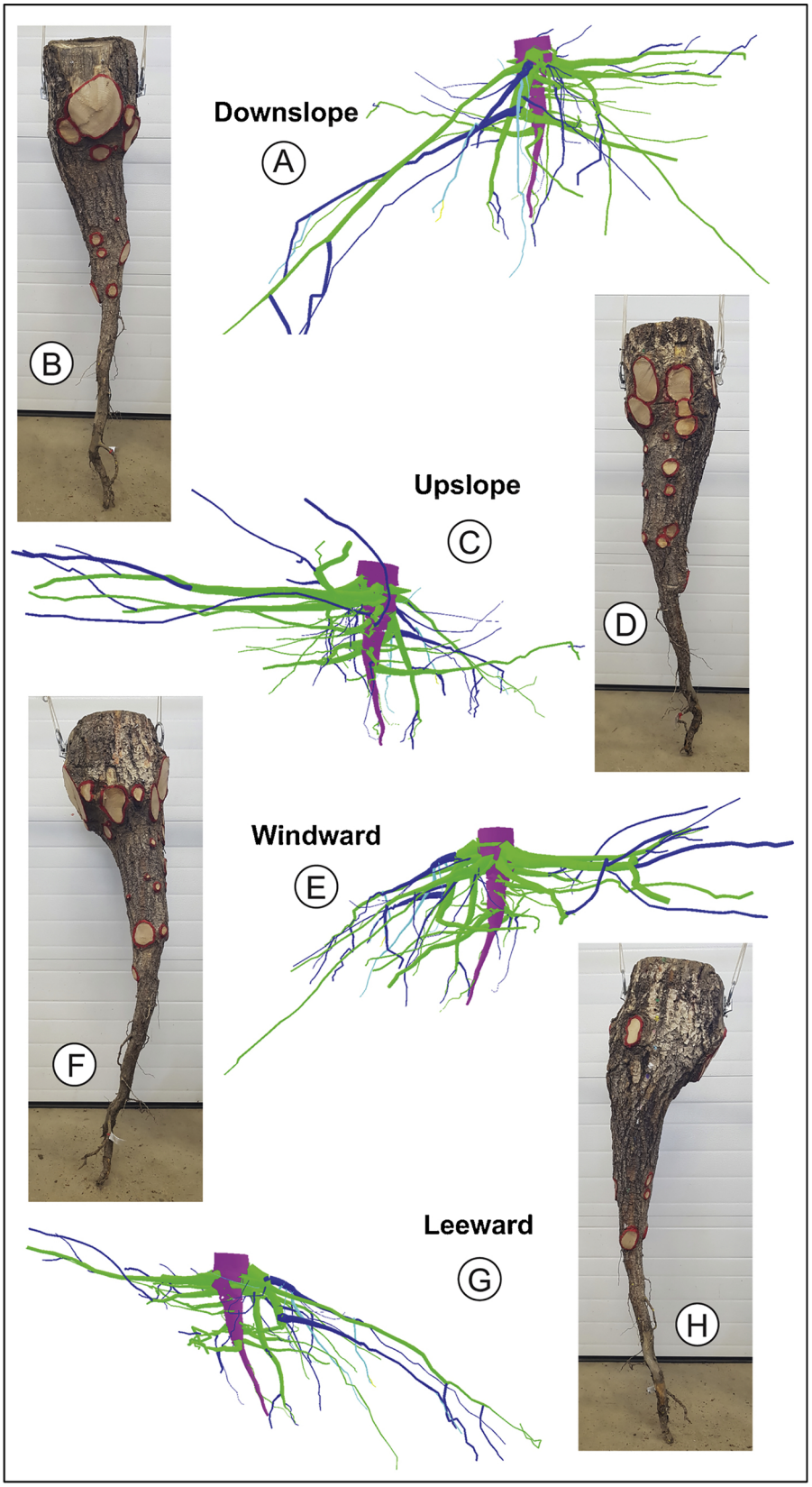

Fig. 3. Root hierarchy was reconstructed for each quadrant using the AMAPmod software. The taproot appears pink, first-order lateral roots emerging from the taproot are green, second-order roots are dark blue, and third-order roots are light blue. Panels A, C, E, and G have the root system oriented so that the downslope, upslope, windward, and leeward quadrants, respectively, are shown. Panels B, D, F, and H, oriented the same way as the root reconstructions, show the cross sectional areas for each first-order lateral root where it attached to the taproot.

Table 3
Lengths and volumes of first-, second-, and third-order lateral roots of a 32-year-old *Pinus ponderosa* at two soil depths (0–30 and 30–60 cm) and four quadrants (downslope, upslope, windward, and leeward) as determined by low magnetic digitizing and AMAPmode software.

Trait	Quadrant	Root order					
		First		Second		Third	
		Soil depth (cm)					
		< 30	> 30	< 30	> 30	< 30	> 30
Length (cm)							
	Downslope	975	201	1142	132	346	44
	Upslope	37	717	0	539	0	0
	Windward	311	739	60	149	0	0
	Leeward	68	296	46	141	80	96
	Total	1390	1953	1248	961	426	141
Volume (cm^3)							
	Downslope	9502	661	3878	814	353	15
	Upslope	1524	4392	0	609	0	0
	Windward	4576	4035	43	113	0	0
	Leeward	35	1168	6	231	20	79
	Total	15637	10257	3927	1767	374	94

necessary to account for ring eccentricity.

In this study we did not investigate the organization of cell walls and therefore cannot demonstrated that the reaction wood we observed is comparable to compression wood or normal wood. However, we stained the wood with a 1% phloroglucinol ethanol solution with one drop of 35% HCl to highlight the presence of a greater content of lignin in the cell walls with a darker/reddish zone (Kutscha and Gray, 1972; Kallavus et al., 2015. Presently we prefer to adopt these traditional terms to indicate wood presenting a considerable eccentricity of the annual rings. Therefore, in our samples, we normally have opposite wood (defined by having the minimum width between annual rings and typical normal wood characteristics; Purusatama et al., 2018) and occurring opposite was compression wood, a zone with the greatest widths between annual rings.

3. Results

3.1. Root system architecture

We observed that 83% of the first-order lateral root length present in the downslope quadrant occurred in the 0–30 cm layer (Table 3), whereas in the upslope quadrant 95% of the first-order root length occurred at depths exceeding 30 cm. For the windward and leeward quadrants, the greatest values for first-order root length were also at a depth of more than 30 cm. Values for second- or third-order lateral roots followed this same pattern. Summed across all four quadrants, 60% of the second- and third-order lateral root length occurred in the upper 30 cm of soil.

First-order lateral root volume in the downslope and upslope quadrants followed the root length pattern: 93% of the total downslope volume occurred in the upper 30 cm of the soil profile whereas 70% of the upslope volume was found below 30 cm. In the windward quadrant at the lower depth, only 40% of the root volume was present, whereas in the leeward quadrant this rooting depth had 97% of the volume. For the second- and third-order lateral roots, the most root volume was found in the upper 30 cm of soil in the downslope quadrant, whereas for the other quadrants the highest percentage was found below 30 cm.

Our data showed that, overall, values for root length and volume were fairly similar regardless of analysis technique (i.e. AQ or EQ) whereas considerable differences sometimes emerged when comparing the two types of measurements within a quadrant (Table 4). For example, in the upslope quadrant, EQ values for first-order length and volume were about 2X those for AQ. About 90% of the total cross sectional area of the downslope quadrant occurs in the upper 30 cm of the taproot (data not shown). Moreover, 43% of the total cross sectional area for the tree occurs in the downslope quadrant (Table 4) being about 25%, 2.5X, and 8X greater than the upslope, windward, and leeward quadrants, respectively.

Table 4
Lengths and volumes of first-, second-, and third-order lateral roots of a 32-year-old *Pinus ponderosa* in four quadrants (downslope, upslope, windward, and leeward) as determine by low magnetic digitizing and AMAPmode software (AQ) or by hand-measurements (EQ). The AQ method assigned root values to the quadrants where the root segment was present while the EQ measurements assigned the root values of the entire root (i.e. first- and second-order) to the quadrant where the first-order root emanated from the taproot. Cross sectional area is the area of the junction of the first-order lateral root to the taproot.

Trait	Quadrant	Root order				
		First		Second		Cross sectional area (cm^2)
		AQ	EQ	AQ	EQ	EQ
Length (cm)						
	Downslope	1176	909	1274	931	240
	Upslope	754	1244	539	519	192
	Windward	1050	767	209	336	96
	Leeward	364	163	187	16	29
	Total	3344	3083	2209	1802	557
Volume (cm^3)						
	Downslope	10163	10271	4692	5799	
	Upslope	5917	10811	609	950	
	Windward	8611	8712	156	135	
	Leeward	1203	1200	237	3	
	Total	25894	30994	5694	6887	

Most first-, second- and third-order lateral roots emanate from the taproot in the downslope quadrant (Fig. 3A and B). In addition, the shallow lateral root presenting the largest cross sectional area (Table 4) was in the downslope quadrant; after a few centimeters its growth angle changes to a sinker root and it deviates from its originating quadrant elongating into the windward quadrant (Fig. 3B). Several second- and third-order lateral roots branched from this root to become sinker roots or to invade a different quadrant (blue and light-blue roots in Fig. 3A).

Fig. 3C shows the growth direction of lateral roots in the upslope quadrant. Unlike the downslope quadrant, the cross sectional area formed by the first-order roots is more diffuse, despite the fact that most of the cross sectional areas are located in the upper 30 cm of the taproot (Fig. 3D). Fig. 3E and G shows lateral roots emanating in the windward and leeward quadrants, respectively. A visual comparison clearly shows the number of roots emanating from the taproot is lower than that in the downslope and upslope quadrants. Only a low amount of cross sectional area occurred in the leeward quadrant (Fig. 3H).

3.2. Tree-ring analysis

Temporal and spatial emission of first-order lateral roots from each quadrant of the taproot is shown in Fig. 4. Most first-order lateral roots originate in the upper 60 cm of taproot length, with about half originating in the uppermost 30 cm. In the downslope, upslope, and windward quadrants, the 30–60 cm taproot depth had more lateral roots characterized by a younger age in respect to the taproot, and these lateral roots were never found to be in a decreasing age order (i.e. from older to younger). The leeward quadrant had no lateral roots younger than the taproot at their relative junction points. Similar to first-order lateral roots, the age of second- and third-order lateral roots was often lower than the age of their relative parental root measured at the branching junction (Fig. 5).

All first-order lateral roots displayed compression wood with

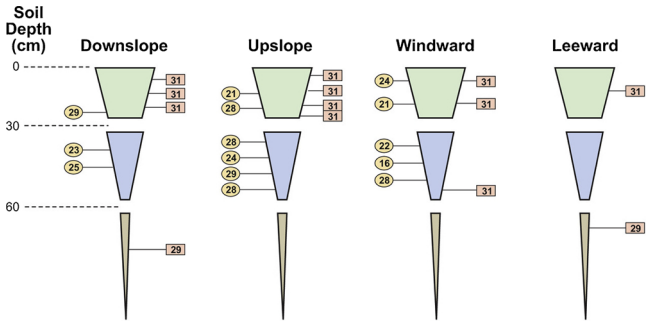

Fig. 4. Tree-ring sequencing of first-order lateral roots emanating from the taproot at three depths (0–30, 30–60, and > 60 cm) for each quadrant (downslope, upslope, windward, and leeward). Rectangles and circles contain the number of growth rings (i.e. age) observed at their junction with the taproot, and are accurate for topology along the taproot axis. Rectangles are for first-order lateral roots for which age coincides exactly with the age of the taproot found at their relative junction points, whereas circles represent the ages of first-order lateral roots when ages did not coincide.

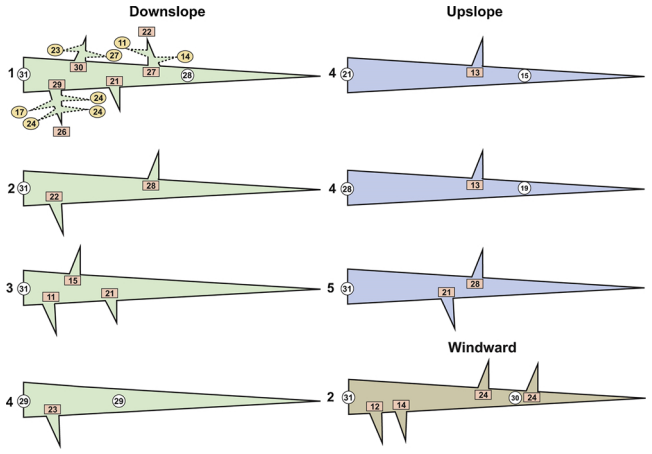

Fig. 5. This schematic shows a number of lateral roots presented as elongated triangles. Although depictions are accurate for order category, topology, and growth direction, they have no relation to actual length, volume, or diameter. Long triangles represent first-order lateral roots. The number at the left side of each first-order lateral root indicates its branching position (moving downward) along the taproot axis and numbers in circles indicate the number of growth rings (i.e. age) at the tap root and along the first-order lateral root axis. The smaller triangles branching from the first-order lateral roots represent second-order lateral roots whereas dotted triangles represent third-order lateral roots. The number in the squares at the base (second-order) or at the end and in circles (third-order) of each branching point are the number of growth rings of the respective roots. The number in the squares at the tips of second-order lateral roots are the number of annual rings beyond the point of initiation of the third-order lateral roots.

considerable eccentricity oriented upward (Fig. 6). Most of the roots showed a T-beam shape while the I-beam shape was observed only in the leeward quadrant (Fig. 6). As our tree-ring analysis extended along the entire length of the root axis, we found that outside the zone of rapid taper the direction of the compression wood changed. In respect to its initial upward direction (i.e. toward the soil surface) we sometimes found a complete inversion with the compression wood directed downward (i.e. away from the soil surface) (Fig. 7A). Finally, at a distance along the axis when the root was no longer undergoing appreciable taper, eccentricity was absent. We also observed that eccentricity can change from upward to sideward when the same root changed growth quadrants from downslope to windward (Fig. 7B).

4. Discussion

Trees in our study formed rigid, cage-like root structures similar to *P. pinaster* (Danjon et al., 2005). This was likely due to our low cohesion frictional soil (Johnson et al., 2007) that allowed the taproot and sinkers to grow straight and deep, and downslope soil hydrological properties that influenced the juvenile developmental stage and shaped future root spatial displacement (Ghestem et al., 2011). Thus, we infer that our RSA description represents the “ground truth” (Clark et al., 2011) development of a 32-year-old *P. ponderosa* tree growing on a steep slope with a volcanic ash-cap soil. In our study, the taproot length was nearly 3X the width of the zone of rapid taper, suggesting that the unimpeded taproot is the major component governing anchorage (Coutts, 1983; Yang et al., 2014, 2016). In this scenario, the taproot provides mechanical anchorage similar to that of a deep stake planted in the soil, guyed by shallow lateral roots (Ennos, 1993; Fourcaud et al., 2008).

Using AMAPmode, our data revealed an uneven distribution of roots in the four quadrants, with the greatest length and volume values in the downslope quadrant, suggesting that, among all the loading forces, the active force downslope requires the strongest mechanical reaction to avoid uprooting. It is reasonable to suggest that the mechanical slope-loading forces could have affected the downslope roots with compressive forces whereas those upslope faced tension forces (Di Iorio et al., 2005). The mechanical role of lateral roots deployed in the downslope quadrant is probably played by their considerable bending stiffness (i.e. product of the elastic modulus of the beam material and the area moment of inertia of the beam cross section). Indeed, according to Coutts (1983), stiffness of a circular beam is related to the fourth power of its diameter, which means that a root with a large cross sectional area will be much stiffer than two roots with the same cumulative cross sectional area.

Volume of lateral roots in the windward quadrant exceeded that of the upslope quadrant, suggesting that wind loading forces are more active than those required to counteract tension forces associated with slope. Moreover, the presence of loading forces due to wind likely explain the higher length and volume values in our windward quadrant compared to the leeward quadrant. These findings, similar to those for *Picea sitchensis* (Nicoll et al., 2006), suggest a root response to dissipate wind-mechanical forces into the soil. Length values in the upslope and windward quadrants were similar, contrasting with Stokes et al. (1995) who reported thinner and more branched roots per unit area of soil on the windward sides of trees. The mechanical efficiency of a root does not, however, depend exclusively on its diameter; Genet et al. (2005) suggest that root tensile strength increases with decreasing diameter.

We observed different values for length and volume depending on the method used to attribute roots to the quadrants. AMAPmode (AQ in Table 2; output based on the physical location of the root segments regardless of its emission point), yielded higher values for first-order lateral roots in all quadrants except upslope, whereas attributing the entire root to the quadrant where the emission is located (EQ in Table 2) yielded the opposite. For volume, upslope values based on AQ are much lower than those determined by EQ. These results highlight that after its emission from the taproot, each first-order lateral root may continue its growth in a different quadrant due to external factors. Our understanding of this phenomenon could be improved if future research work also included a tree-ring-analysis approach to determine if lateral roots found at the adult stage were the same ones present at the seedling stage.

Several authors report the occurrence of discontinuous annual rings indicative of discontinuous wood production (references in Wrońska-Wałach et al., 2016). We noted discontinuous rings more frequently in second- and third-order roots than in first-order roots. While the mechanism responsible for discontinuous rings remains unknown, it may be the result of different cell division activity along the vascular cambium circumference caused by mechanical stress, similar to how this

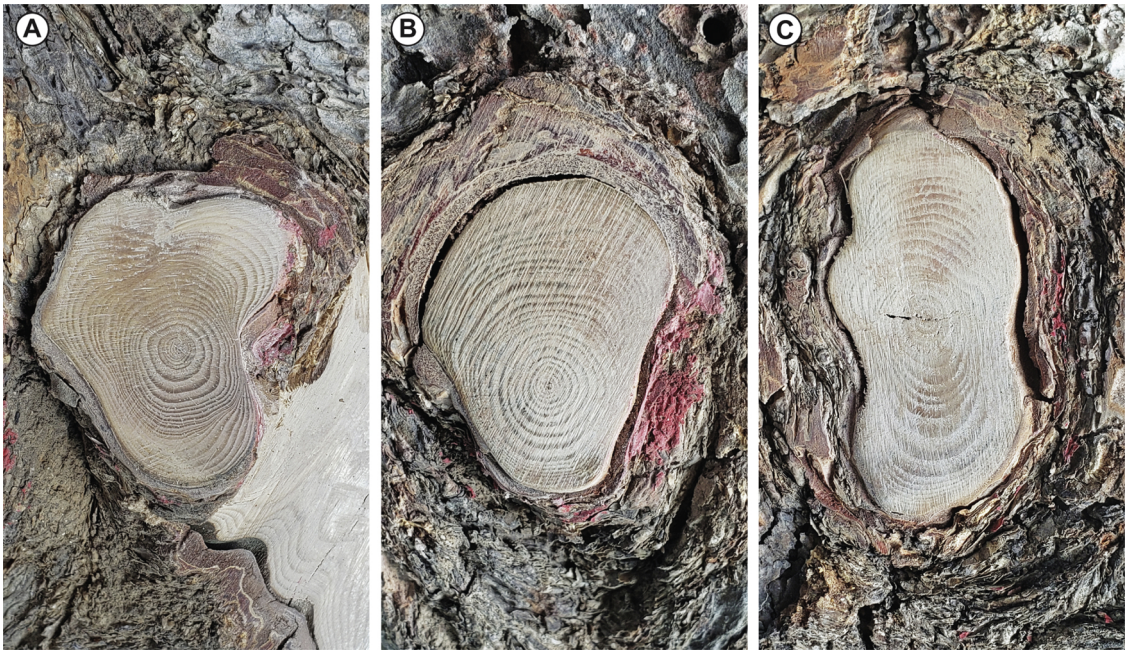

Fig. 6. Cross sectional areas (prior to fine sanding) of the junctions of first-order lateral roots with the taproot display compression wood with considerable eccentricity oriented upward regardless of quadrant. Examples of T-beam (A and B; windward quadrant) and I-beam (C; leeward quadrant) structures.

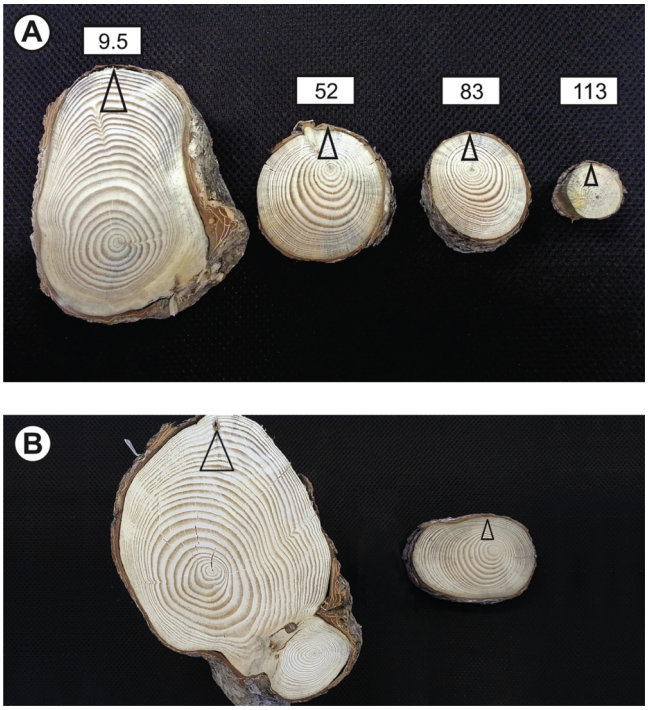

Fig. 7. Triangles on cross sections indicate the topological upward (i.e. toward the soil surface) positions of the roots *in situ*. Cross sections obtained along the 143-cm root axis of a first-order lateral root in the windward quadrant (A).Values in boxes are the distances (cm) of each cross section from the taproot. The second, third, and fourth cross sections are outside the zone of rapid taper. The eccentricity of the annual rings is upward in the first cross section but downward in the second and third cross sections. In the fourth cross section, well beyond the zone of rapid taper, eccentricity is absent. Cross sections of a first-order lateral root in the downslope quadrant (B). The left section is in the downslope quadrant and shows upward eccentricity, but when the root turns and enters the windward quadrant (right section), the eccentricity changes direction.

stress is responsible for asymmetric annual ring distribution observed in large-diameter roots (see below). We observed that the smaller-diameter roots outside the zone of rapid taper sometimes showed several discontinuous annual rings, suggesting they could be subjected to mild mechanical forces.

Asymmetric wood production in our roots reflects the presence of reaction wood (Fischer et al., 2019), analogous with the mechanism responsible for reorienting the stem axis (Sinnott, 1952). Indeed, Groover (2016) suggests that reaction wood is central to concepts of mechanical design and adaptive growth that describe how tree stem and branches respond to environmental stresses. Our data show that despite the likely qualitative and quantitative differences in mechanical forces (compression and tension) active in the various quadrants of our root system, the observed response was always formation of annual ring eccentricity oriented upward (i.e. toward soil surface), at least in the zone of rapid taper. Similarly, Du and Yamamoto (2007) demonstrated that reaction wood in branches always forms on the side where it will serve to reestablish the equilibrium position; in their research, the vascular cambium seems to respond by producing more wood in the direction where tissue perceives the gravity stimulus. Fayle (1968) observed root annual rings with downward eccentricity when soil erosion exposed them to the air, perhaps because exposure to air induces anatomical modifications in wood increments between the upper and lower part of the central root axis. In *Larix decidua*, Gärtner et al., 2006 reported that roots growing 20 cm below the soil surface lacked differences between and early- and late-wood whereas closer to the surface these differences were more evident. In our roots, the presence of soil might reduce the gravity stimulus whereas tension and compression forces could have the main influence, similar to results for *Populus* (Stokes and Mattheck, 1996) where increases in compression strength on the underside of lateral roots induced a radial growth reduction as consequence of the weight of the tree pressing the lateral root on to the soil. Given that compression wood in our roots was always formed in the upward direction, we suggest that the mechanical stimulation and/or inhibition of vascular cambium initials cells can take place in the upper and lower side of the root, respectively. This is independent of the type of mechanical force (i.e. compressive or tension).

Distinguishing the effects of different factors (i.e. mechanical forces

or gravity) responsible for inducing wood response in stems, branches, or roots remains a challenging objective (Lopez et al., 2014). Our finding that the compression wood orientation along the axis of first-order lateral roots within the zone of rapid taper changed when the root grew outside this zone may be explained as a root response to different dominant factors along its length.

Indeed, Coutts et al. (1999) suggest that the change in reaction wood direction coinciding with the exit from the root cage could be the response to the diminished need of root stiffness. Our finding also concurs with Nicoll and Dunn (2000) who concluded modifications in radial growth of shallow structural roots of *P. sitchensis* were attributed to a response to frequent and strong wind loading. Similar to our findings, White (1965) showed the formation of a spiral compression wood that began an up-soil orientation but changed to a down-soil direction outside the zone of rapid taper. Also, Gärtner (2007) found that the anatomical structure of roots changes due to their function and depth below the soil surface. Finally, Stokes and Mattheck (1996) found that in the root system of a tree with a large taproot (similar to our trees), the compression and bending strength acting on lateral roots decreased with increasing distance from the branching point. Considered together, this literature suggests that in our case the opposite side of eccentricity (opposite wood) could be involved in root resistance against the compression forces, whereas the upper-side could respond to tension forces. If so, then the same root would be able to respond to two different mechanical forces. Because eccentricity direction is the same in all our quadrants, this suggests that the root system is prepared to respond to tension or compression forces from whatever direction these inducing forces arrive. The change in quality and quantity of the inducing factor would explain why in our root 1) the amount of compression wood decreases along the root axis until the eccentricity is completely eliminated, and 2) the orientation of the annual ring eccentricity changes at a certain distance from the branching point. Until a definitive explanation is available, we suggest that the compression wood observed in our roots responds to a variation of the direction of the mechanical forces active on the vascular cambium and we reasonably exclude gravity as a primary factor.

RSA studies normally adopt a static approach, neglecting to monitor the dynamics of lateral root development (Dubrovsky and Forde, 2012) in stark contrast with the growing awareness that the RSA at a specific time represents the sum of root system adaptation to local situations (Füllner et al., 2011). We therefore reasonably speculate that continuously changing environmental conditions (e.g. wind, slope conditions, and changes in self-loading weight of shoots) require a spatial change in the distribution of root system biomass to satisfy mutable needs. In a woody root, however, the primary structure to initiate new roots is found in the proximal few millimeters of its extension, whereas the remaining length is characterized by a secondary structure with an increasing number of annual rings of wood tissue going from proximal to distal position (Evert, 2006). Enumeration of these rings is an accepted, accurate way to determine root age (Krause and Eckstein, 1993; Krause and Morin, 1999). Our data demonstrate, however, that some distal lateral roots have fewer annual rings than would be expected by the annual ring count of the parental root at the branching point. In other words, annual rings were added to the parental root before the new distal root developed, and the difference in the number of annual rings between the new and parental roots would indicate how many years later that particular lateral root was emitted. Thus, parental roots formed new primordia in the absence of pericycle tissue (i.e. with the presence of cambial tissue) (see also Chiatante et al., 2010; Baesso et al., 2018). What remains to discern is whether or not this root development responds to the same regulatory mechanisms associated with the pericycle. Furthermore, our observation that new lateral root formation occurs at a later stage of root development suggests an adaptive response to improve resistance to mechanical loading forces active in the quadrant where this new root is placed, although we cannot exclude the possibility that new roots formed to improve the nutritional role in a certain soil direction.

5. Conclusions

In conclusion, our work with *P. ponderosa* revealed that 1) first-order lateral roots show similar patterns of annual ring eccentricity, suggesting roots have an ability to respond to different mechanical forces at their onset; 2) on a steep slope, more root resources are allocated to the downslope quadrant, followed by the windward quadrant; 3) larger cross sectional areas at the point of attachment of lateral roots to the taproot in the downslope quadrant suggests these shallow roots play an important role in tree anchorage; 4) roots change growth direction in response to mechanical forces; 5) all the most important roots involved in anchorage presented compression wood formation, and the orientation of compression wood shifted from an upward orientation to downward orientation moving from the zone of rapid taper outward; and 6) employing a tree-ring-analysis approach, the ages of first-, second-, and third-order lateral roots were often lower than the age of their relative parental roots measured at the branching junction, indicating that new lateral roots can be produced by a parental root at any developmental stage, at any location along the parental root axis, and whenever necessary to modify root system architecture in response to environmental stimuli. Together, these findings support our hypotheses that trees continuously adjust root spatial deployment in response to environmental conditions through emission of new lateral roots, change of growth direction, and production of reaction wood.

Declaration of competing interests

The authors declare that they have no competing interests.

Acknowledgments

We thank Dr. Frédéric Danjon of the French National Institute for Agricultural Research (INRA) of Bordeaux for help with AMAPmode system, and Jim Marin for some of the visualizations in this paper. This study was supported by the University of Insubria, the University of Molise, the U.S. Department of Agriculture Forest Service (USFS) Rocky Mountain Research Station, and the USFS National Center for Reforestation, Nurseries, and Genetic Resources.

References

Alméras, T., Clair, B., 2016. Critical review on the mechanisms of maturation stress generation in trees. J. R. Soc. Interface 13, 20160550, https://doi.org/10.1098/rsif.2016.0550.

Anten, N.P.R., Schieving, F., 2010. The role of wood mass density and mechanical constraints in the economy of tree architecture. Am. Nat. 175 (2), 250–260. https://doi.org/10.1086/649581.

Atkinson, J.A., Pound, M.P., Bennett, M.J., Wells, D.M., 2019. Uncovering the hidden half of plants using new advances in root phenotyping. Curr. Opin. Biotechnol. 55, 1–8. https://doi.org/10.1016/j.copbio.2018.06.002.

Baesso, B., Chiatante, D., Terzaghi, M., Zenga, D., Nieminen, K., Mahonen, A.P., Siligato, R., Helariutta, Y., Scippa, G.S., Montagnoli, A., 2018. Transcription factors PRE3 and WOX11 are involved in the formation of new lateral roots from secondary growth taproot in *A. thaliana*. Plant Biol. Stuttg. (Stuttg) 20, 426–432. https://doi.org/10.1111/plb.12711.

Böhm, W., 1979. Methods of Studying Root Systems. Springer, Berlin.

Chave, J., Coomes, D., Jansen, S., Lewis, S.L., Swenson, N.G., Zanne, A.E., 2009. Towards a worldwide wood economics spectrum. Ecol. Lett. 12, 351–366. https://doi.org/10.1111/j.1461-0248.2009.01285.x.

Chiatante, D., Beltotto, M., Onelli, E., Di Iorio, A., Montagnoli, A., Scippa, G.S., 2010. New branch roots produced by vascular cambium derivatives in woody parental roots of *Populus nigra* L. Plant Biosyst. 144, 420–433. https://doi.org/10.1080/11263501003718612.

Chiatante, D., Terzaghi, M., Scippa, G.S., Montagnoli, A., 2019. Advances in understanding root development in forest trees, ch. 2. In: Stanturf, J.A. (Ed.), Sustainable Management of Boreal and Temperate Forests. Burleigh Dodds Science Publishing, Cambridge UK.

Clark, R.T., MacCurdy, R.B., Jung, J.K., Shaff, J.E., McCouch, S.R., Aneshansley, D.J., Kochian, L.V., 2011. Three-dimensional root phenotyping with a novel imaging and software platform. Plant Physiol. 156, 455–465. https://doi.org/10.1104/pp.110.

169102.
Colombi, T., Kirchgessner, N., Le Marié, C.A., York, L.M., Lynch, J.P., Hund, A., 2015. Next generation shovelomics: set up a tent and REST. Plant Soil 388, 1–20. https://doi.org/10.1007/s11104-015-2379-7.
Cooper, S.T., Neiman, K.E., Steele, R., Roberts, D.W., 1987. Forest Habitat Types of Northern Idaho: A Second Approximation. U.S. Department of Agriculture, Forest Service, Intermountain Research Station, Ogden, Utah General Technical Report INT–236. 135 p.
Coutts, M.P., 1983. Root architecture and tree stability. Plant Soil 71, 171–188. https://doi.org/10.1007/BF02182653.
Coutts, M.P., Nielsen, C.C.N., Nicoll, B.C., 1999. The development of symmetry, rigidity and anchorage in the structural root system of conifers. Plant Soil 217, 1–15. https://doi.org/10.1023/A:1004578032481.
Danjon, F., Stokes, A., Bakker, M., 2013. Root systems of woody plants, ch. 29. In: Eshel, A., Beeckman, T. (Eds.), Plant Roots, the Hidden Half, 4th ed. CRC Press, https://doi.org/10.1201/b14550-34. 848 pp.
Danjon, F., Fourcaud, T., Bert, D., 2005. Root architecture and wind-firmness of mature *Pinus pinaster*. New Phytol. 168, 387–400. https://doi.org/10.1111/j.1469-8137.2005.01497.x.
De Zio, E., Trupiano, D., Montagnoli, A., Terzaghi, M., Chiatante, D., Gross, A., Marra, M., Scaloni, A., Scippa, G.S., 2016. Poplar woody taproot under bending stress: the asymmetric response of the convex and concave sides. Ann. Bot. 118, 865–883. https://doi.org/10.1093/aob/mcw159.
Di Iorio, A., Lasserre, B., Scippa, G.S., Chiatante, D., 2005. Root system of *Quercus pubescens* trees growing on different sloping conditions. Ann. Bot. 95, 351–361. https://doi.org/10.1093/aob/mci033.
Di Iorio, A., Lasserre, B., Scippa, G.S., Chiatante, D., 2007. Pattern of secondary thickening in a *Quercus cerris* root system. Tree Physiol. 27, 407–412. https://doi.org/10.1093/treephys/27.3.407.
Du, S., Yamamoto, F., 2007. An overview of the biology of reaction wood formation. J. Integr. Plant Biol. 49, 131–143. https://doi.org/10.1111/j.1744-7909.2007.00427.x.
Donaldson, L.A., Singh, A.P., 2016. Reaction wood, ch. 6. In: Kim, Y.S., Funada, R., Singh, A.P. (Eds.), Secondary Xylem Biology—Origins, Functions, and Applications. Elsevier, Inc., pp. 93–110.
Dubrovsky, J.G., Forde, B.G., 2012. Quantitative analysis of lateral root development: pitfalls and how to avoid them. Plant Cell 24, 4–14. https://doi.org/10.1105/tpc.111.089698.
Dumroese, R.K., Terzaghi, M., Chiatante, D., Scippa, G.S., Lasserre, B., Montagnoli, A., 2019. Functional traits of *Pinus ponderosa* coarse-roots in response to slope conditions. Front. Plant Sci. 10, 947, https://doi.org/10.3389/fpls.2019.00947.
Dupuy, L., Gregory, P.J., Bengough, A.G., 2010. Root growth models: towards a new generation of continuous approaches. J. Exp. Bot. 61, 2131–2143. https://doi.org/10.1093/jxb/erp389.
Ennos, A.R., 1993. The scaling of root anchorage. J. Theor. Biol. 161, 61–75. https://doi.org/10.1006/jtbi.1993.1040.
Evert, R.F., 2006. Esau's Plant Anatomy, Meristems, Cells, and Tissues of the Plant Body: Their Structure, Function, and Development, 3rd ed. John Wiley & Sons, Inc., New Jersey. https://doi.org/10.1002/0470047380. 601 pp.
Fayle, D.C.F., 1968. Radial growth in tree roots: distribution, timing, anatomy. Faculty of Forestry, University of Toronto, Toronto, Ontario. Tech. Rep. No. 9 183 pp.
Fayle, D.C.F., 1975. Distribution of radial growth during the development of red pine root systems. Can. J. For. Res. 5, 608–625. https://doi.org/10.1139/x75-088.
Fayle, D.C.F., 1976. Stem sway affects ring width and compression wood formation in exposed root bases. For. Sci. 22, 193–194. https://doi.org/10.1093/forestscience/22.2.193.
Fischer, U., Kucukoglu, M., Heliarutta, Y., Bhalerao, R., 2019. The dynamics of cambial stem cell activity. Annu. Rev. Plant Biol. 70, 293–319. https://doi.org/10.1146/annurev-arplant-050718-100402.
Fourcaud, T., Ji, J.N., Zhang, Z.Q., Stokes, A., 2008. Understanding the impact of root morphology on overturning mechanisms: a modelling approach. Ann. Bot. 101, 1267–1280. https://doi.org/10.1093/aob/mcm245.
Füllner, K., Temperton, V.M., Rascher, U., Jahnke, S., Rist, R., Schurr, U., Kuhn, A.J., 2011. Vertical gradient in soil temperature stimulates development and increases biomass accumulation in barley. Plant Cell Environ. 35, 884–892. https://doi.org/10.1111/j.1365-3040.2011.02460.x.
Gärtner, H., 2006. The applicability of roots in dedrogeomorphology. In: In: Schleser, G., Winiger, M., Bräuning, A., Gärtner, H., Helle, G., Jansma, E., Neuwirth, B., Treydte, K. (Eds.), TRACE - Tree Rings in Archaeology, Climatology and Ecology 1. pp. 120–124.
Gärtner, H., 2007. Tree roots - methodological review and new development in dating and quantifying erosive processes. Geomorphology 86, 243–251. https://doi.org/10.1016/j.geomorph.2006.09.001.
Genet, M., Stokes, A., Salin, F., Mickovski, S.B., Fourcaud, T., Dumail, J.-F., van Beek, R., 2005. The influence of cellulose content on tensile strength in tree roots. Plant Soil 278, 1–9. https://doi.org/10.1007/s11104-005-8768-6.
Ghani, M.A., Stokes, A., Fourcaud, T., 2009. The effect of root architecture and root loss through trenching on the anchorage of tropical urban trees (*Eugenia grandis* Wight). Trees 23, 197–209. https://doi.org/10.1007/s00468-008-0269-9.
Ghestem, M., Sidle, R.C., Stokes, A., 2011. The influence of plant root systems on subsurface flow: implications for slope stability. BioScience 61, 869–879. https://doi.org/10.1525/bio.2011.61.11.6.
Godin, C., Caraglio, Y., 1998. A multiscale model of plant topological structures. J. Theor. Biol. 191, 1–46. https://doi.org/10.1006/jtbi.1997.0561.
Godin, C., Costes, E., Caraglio, Y., 1997. Exploring plant topological structure with the AMAPmod software: an outline. Silva Fenn. 31, 357–368. https://doi.org/10.14214/sf.a8533.
Groover, A., 2016. Gravitropisms and reaction woods of forest trees - evolution, functions and mechanisms. New Phytol. 211https://doi.org/10.1111/nph.13968. 790–80.
Hathaway, R.L., Penny, D., 1975. Root strength in some *Populus* and *Salix* clones. N.Z. J. Bot. 13, 333–344. https://doi.org/10.1080/0028825X.1975.10430330.
Hitz, O.M., Gärtner, H., Heinrich, I., Monbaron, M., 2008. Wood anatomical changes in roots of European ash (*Fraxinus excelsior* L.) after exposure. Dendrochronologia 25, 145–152. https://doi.org/10.1016/j.dendro.2007.03.005.
Iyer-Pascuzzi, A.S., Symonova, O., Mileyko, Y., Hao, Y., Belcher, H., Harer, J., Weitz, J.S., Benfey, P.N., 2010. Imaging and analysis platform for automatic phenotyping and trait ranking of plant root systems. Plant Physiol. 152, 1148–1157. https://doi.org/10.1104/pp.109.150748.
Ji, J., Kokutse, N., Genet, M., Fourcaud, T., Zhang, Z., 2012. Effect of spatial variation of tree root characteristics on slope stability. A case study on black locust (*Robinia pseudoacacia*) and arborvitae (*Platycladus orientalis*) stands on the Loess Plateau, China. Catena 92, 139–154. https://doi.org/10.1016/j.catena.2011.12.008.
Johnson, L.R., Page-Dumroese, D., Han, H.S., 2007. Effects of machine traffic on the physical properties of ash-cap soils. In: Page-Dumroese, D., Miller, R., Mital, J., McDaniel, P., Miller, D. (Eds.), Volcanic-Ash-Derived Forest Soils of the Inland Northwest: Properties and Implications for Management and Restoration. U.S. Department of Agriculture, Forest Service, Rocky Mountain Research Station, Fort Collins, Colorado, pp. 69–82 Proceedings RMRS-P-44.
Kallavus, U., Kärner, Kr., Kärner, Kä., Elomaa, M., 2015. Rapid semi-quantitative determination of aspen lignin in lignocellulosic products. Proc. Est. Acad. Sci. 64 (1), 105–112. https://doi.org/10.3176/proc.2015.1S.06.
Kim, Y.S., Funada, R., Adya, P., 2016. Secondary Xylem Biology: Origins, Functions, and Applications. Academic Press, USA 416 pp.
King, J.S., Thomas, R.B., Strain, B.R., 1996. Growth and carbon accumulation in root systems of *Pinus taeda* and *Pinus ponderosa* seedlings as affected by varying CO_2, temperature, and nitrogen. Tree Physiol. 16, 635–642. https://doi.org/10.1093/treephys/16.7.635.
Krause, C., Eckstein, D., 1993. Dendrochronology of roots. Dendrochronologia 11, 9–23.
Krause, C., Morin, H., 1995. Changes in radial increment in stems and roots of balsam fir (*Abies balsamea* (L.) Mill.) after defoliation by spruce budworm. For. Chron. 71, 747–754.
Krause, C., Morin, H., 1999. Root growth and absent rings in mature black spruce and balsam fir, Quebec, Canada. Dendrochronologia 16/17, 21–35.
Kutscha, N., Gray, J.R., 1972. TB53: the suitability of certain stains for studying lignification in balsam fir, *Abies balsamea* (L.) Mill. University of Maine, Life Sciences and Agriculture Experiment Station Technical Bulletin. 53.
Lombardi, F., Scippa, G.S., Lasserre, B., Montagnoli, A., Tognetti, R., Marchetti, M., Chiatante, D., 2017. The influence of slope on *Spartium junceum* root system: morphological, anatomical and biomechanical adaptation. J. Plant Res. 130, 515–525. https://doi.org/10.1007/s10265-550017-0919-3.
Lopez, D., Tocquard, K., Venisse, J.S., Legue, V., Roeckel-Drevet, P., 2014. Gravity sensing, a largely misunderstood trigger of plant orientated growth. Front. Plant Sci. Plant Physiol. 5, 610, https://doi.org/10.3389/fpls.2014.00610.
Montagnoli, A., Dumroese, R.K., Terzaghi, M., Onelli, E., Scippa, G.S., Chiatante, D., 2019. Seasonality of fine root dynamics and activity of root and shoot vascular cambium in *Quercus ilex* L. forest (Italy). For. Ecol. Manag. 431, 26–34. https://doi.org/10.1007/s10342-014-0814-6.
Nicoll, B.C., Dunn, A.J., 2000. The effects of wind speed and direction on radial growth of structural roots. In: In: Stokes, A. (Ed.), The Supporting Roots of Trees and Woody Plants: Form, Function and Physiology. Developments in Plant and Soil Sciences, vol. 87. Springer, Dordrecht, pp. 219–225. https://doi.org/10.1007/978-94-017-3469-1_21.
Nicoll, B.C., Berthier, S., Achim, A., Gouskou, K., Danjon, F., van Beek, L.P.H., 2006. The architecture of *Picea sitchensis* structural root systems on horizontal and sloping terrain. Trees 20, 701–712. https://doi.org/10.1007/s00468-006-0085-z.
Pagès, L., 2002. Modelling root system architecture. In: Waisel, Y., Eshel, A., Kafkafi, U. (Eds.), Plant Roots: the Hidden Half. Marcel Dekker Pub., pp. 359–382.
Puhe, J., 2003. Growth and development of the root system of Norway spruce (*Picea abies*) in forest stands - a review. For. Ecol. Manag. 175, 253–273. https://doi.org/10.1016/S0378-1127(02)00134-2.
Purusatama, B.D., Kim, Y.K., Jeon, W.S., Lee, J.A., Kim, A.R., Kim, N.H., 2018. Qualitative anatomical characteristics of compression wood, lateral wood, and opposite wood in a stem of *Ginkgo biloba* L. J. Korean Wood Sci. Technol. 46, 125–131. https://doi.org/10.5658/WOOD.2018.46.2.125.
Ruelle, J., 2014. Morphology, anatomy and ultrastructure of reaction wood. In: Gardiner, B., Barnett, J., Saranpää, P., Gril, J. (Eds.), The Biology of Reaction Wood. Springer Series in Wood Science. Springer, Berlin, Heidelberg. https://doi.org/10.1007/978-3-642-10814-3_2.
Schroth, G., 1998. A review of belowground interactions in agroforestry, focusing on mechanisms and management options. Agrofor. Syst. 43, 5–34. https://doi.org/10.1023/A:1026443018920.
Sinnott, E.W., 1952. Reaction wood and the regulation of tree form. Am. J. Bot. 39, 69–78. https://doi.org/10.2307/2438096.
Soil Survey Staff, 2013. https://soilseries.sc.egov.usda.gov/OSD_Docs/V/VASSAR.html. (Accessed 24 January 2019).
Sorgonà, A., Proto, A.R., Abenavoli, L.M., Di Iorio, A., 2018. Spatial distribution of coarse root biomass and carbon in a high-density olive orchard: effects of mechanical harvesting methods. Trees 32, 919–931. https://doi.org/10.1007/s00468-018-1686-z.
Stokes, A., Mattheck, C., 1996. Variation of wood strength in tree roots. J. Exp. Bot. 47, 693–699. https://doi.org/10.1093/jxb/47.5.693.
Stokes, A., Fitter, A.H., Coutts, M.P., 1995. Responses of young trees to wind and shading - effects on root architecture. J. Exp. Bot. 46, 1139–1146. https://doi.org/10.1093/jxb/46.9.1139.

Stokes, A., Atger, C., Bengough, A.G., Fourcaud, T., Sidle, R.C., 2009. Desirable plant root traits for protecting natural and engineered slopes against landslides. Plant Soil 324, 1–30. https://doi.org/10.1007/s11104-009-0159-y.

Terzaghi, M., Di Iorio, A., Montagnoli, A., Baesso, B., Scippa, G.S., Chiatante, D., 2016. Forest canopy reduction stimulates xylem production and lowers carbon concentration in fine roots of European beech. For. Ecol. Manag. 379, 81–90. https://doi.org/10.1016/j.foreco.2016.08.010.

van Gelder, H.A., Poorter, L., Sterck, F.J., 2006. Wood mechanics, allometry, and life-history variation in a tropical tree community. New Phytol. 171, 367–378. https://doi.org/10.1111/j.1469-8137.2006.01757.x.

Wenny, D.L., Dumroese, R.K., 1987. A Growing Regime for Containerized Ponderosa Pine Seedlings. University of Idaho, Idaho Forest, Wildlife and Range Experiment Station, Moscow, ID *Bulletin 43*. 9 p.

Wenny, D.L., Liu, Y., Dumroese, R.K., Osborne, H.L., 1988. First year field growth of chemically root pruned containerized seedlings. New For. 2, 111–118. https://doi.org/10.1007/BF00027762.

Western Regional Climate Center, 2019. https://wrcc.dri.edu. (Accessed 1 October 2019).

Westing, A.H., 1965. Formation and function of compression wood in gymnosperms. II. Bot. Rev. 34, 51–78. https://doi.org/10.1007/BF02858621.

White, D.J.B., 1965. The anatomy of reaction tissues in plants. In: Carthy, J.D., Duddington, C.L. (Eds.), Viewpoints in Biology, IV, Butterworth London, pp. 54–82.

Wistuba, M., Malik, I., Gärtner, H., Kojs, P., Owczarek, P., 2013. Application of eccentric growth of trees as a tool for landslide analyses: the example of *Picea abies* Karst. In the Carpathian and Sudeten Mountains (Central Europe). Catena 111, 41–55. https://doi.org/10.1016/j.catena.2013.06.027.

Wrońska-Wałach, D., Sobucki, M., Buchwał, A., Gorczyca, E., Korpak, J., Wałdykowski, P., Gärtner, H., 2016. Quantitative analysis of ring growth in spruce roots and its application towards a more precise dating. Dendrochronologia 38, 61–71. https://doi.org/10.1016/j.dendro.2016.03.009.

Yang, M., Défossez, P., Danjon, F., Fourcaud, T., 2014. Tree stability under wind: simulating uprooting with root breakage using a finite element method. Ann. Bot. 114, 695–709. https://doi.org/10.1093/aob/mcu122.

Yang, M., Défossez, P., Danjon, F., Dupont, S., Fourcaud, T., 2016. Which root architectural elements contribute the best to anchorage of *Pinus* species? Insights from in silico experiments. Plant Soil 411, 275–291. https://doi.org/10.1007/s11104-016-2992-0.

Zobel, R.W., Waisel, Y., 2010. A plant root system architectural taxonomy: a framework for root nomenclature. Plant Biosyst. 144, 507–512. https://doi.org/10.1080/11263501003764483.